

Cite this: DOI: 10.1039/c3dt51226f

Ligand dissociation/recoordination in fluorescent ionic zinc–salicylideneimine compounds: synthesis, characterization, photophysical properties, and ^1H NMR studies†

Ho-Wen Chiang, Yo-Ting Su and Jing-Yun Wu*

A series of ionic zinc–salicylideneimine compounds, $[\text{HNEt}_3][\text{Zn}(\text{L})\text{Cl}_2]$ ($\text{L} = \text{sal}^{\text{H}}\text{-4-CN}$, **1**; $\text{sal}^{\text{Cl}}\text{-4-CN}$, **2**; $\text{sal}^{\text{Br}}\text{-4-CN}$, **3**; $\text{sal}^{\text{OMe}}\text{-4-CN}$, **4**) and $[\text{NEt}_4][\text{Zn}(\text{sal}^{\text{H}}\text{-4-CN})\text{Cl}_2]$ (**5**), have been synthesized and structurally characterized. Compounds **1–5** all display an intense fluorescence band in both solution (methanol, MeOH; acetonitrile, ACN; dimethylsulfoxide, DMSO; dichloromethane, DCM) and solid phases, with a maximum in the region of 515–560 nm and 529–573 nm, respectively. Detailed ^1H NMR and optical spectroscopic studies indicate the occurrence of ligand dissociation and recoordination in **1–4** in solution, leading to an equilibrium between the zinc–salicylideneimine complex species, $[\text{Zn}(\text{L})\text{Cl}_2]^-$, and the salicylideneimine free ligand, HL. The tendency of ligand dissociation is related to the solvent, the concentration, and the substitution of the salicylidene ring. The greatest degree of ligand dissociation is observed for **1–4** when dissolved in noncoordinating, less polar DCM solvent, followed by coordinating, high polar DMSO solvent. The least degree of ligand dissociation occurs in solutions of coordinating, moderately polar MeOH and ACN solvents for **1–3** and **4**, respectively. Dilute solutions are likely characterized by the high degree of ligand dissociation, whereas the equilibrium shifts in favor of the complex $[\text{Zn}(\text{L})\text{Cl}_2]^-$ form at higher concentration. Furthermore, the electron-donating methoxy substitution in the salicylidene ring promotes a high tendency for ligand dissociation, while electron-withdrawing chloro and bromo groups cause the reverse tendency. The ^1H NMR spectrum of **5** shows only one set of proton resonances in the aromatic region corresponding to the complex $[\text{Zn}(\text{sal}^{\text{H}}\text{-4-CN})\text{Cl}_2]^-$ species, indicating that the lack of ammonium proton would protect the complex form from ligand dissociation.

Received 10th May 2013,
Accepted 6th August 2013

DOI: 10.1039/c3dt51226f

www.rsc.org/dalton

Introduction

Salicylideneimine derivatives or imine–phenol Schiff base ligands, which are easily synthesized by the condensation reactions of primary amines and salicylaldehyde or its analogues, are capable of forming stable complexes with certain metal ions through the azomethine nitrogen and phenolato oxygen,¹ giving rise to the most fundamental N,O-chelating system in coordination chemistry.² These metal–salicylideneimine complexes have shown intriguing structural topologies, high thermodynamic stability, excellent catalytic activities, and biological activities as well as good luminescent properties.^{1,3–10}

In addition, metal complexes of functionalized salicylideneimine derivatives can themselves also serve as interesting metalloligands, which may be further coordinated through either additional functionalities or *cis*-oxygen atoms to other metal ions so that new supramolecular materials are constructed.^{11–15} On the other hand, salicylideneimine derivatives have also been reported as successful fluorescent chemosensors for selective detection of various environmentally and biologically relevant metal ions due to the enhanced fluorescence upon interaction with an analyte.^{16,17}

Zinc–salicylideneimine complexes have recently attracted considerable attention for their variegated fluorescence features, which are related to the structures^{9,10b,18} and, specifically, the axial coordination.^{8a,c,10,19} As part of the effort in studying unique salicylideneimine ligands and their complexation chemistry, we report herein the synthesis and characterization of a series of ionic zinc–salicylideneimine compounds, $[\text{HNEt}_3][\text{Zn}(\text{L})\text{Cl}_2]$, displaying good fluorescence properties. These zinc(II) materials would undergo a dissociation process

Department of Applied Chemistry, National Chi Nan University, Nantou 545, Taiwan. E-mail: jyumwu@ncnu.edu.tw; Fax: +886-49-2917956; Tel: +886-49-2910960-4918

†Electronic supplementary information (ESI) available: ^1H NMR, UV-vis, and fluorescence spectra. CCDC 935863–935869. For ESI and crystallographic data in CIF or other electronic format see DOI: 10.1039/c3dt51226f

to give the free neutral form of the HL ligand and an un-identified zinc species in solution, leading to a dynamic equilibrium between ligand dissociation and recoordination. Through detailed ^1H NMR and optical spectroscopic studies, it has been shown that the concentration, the solvent, and the substituent of the ligand play decisive roles in affecting the dissociation/recoordination process, leading to different degrees of dissociation.

Experimental section

Materials and instrumentation

Chemical reagents were purchased commercially and were used as received without further purification. ^1H NMR spectra were recorded on a Bruker AMX-300 Solution-NMR spectrometer. Chemical shifts are reported in parts per million (ppm) with reference to the residual protons of the deuterated solvent. Coupling constants are reported in Hertz (Hz). Mass spectra were recorded with a Bruker Daltonics flexAnalysis matrix-assisted laser desorption/ionization time of flight (MALDI-TOF) mass spectrometer. Infrared (IR) spectra were recorded on a Perkin-Elmer RX1 Fourier transform infrared spectrometer using KBr discs in the 4000–400 cm^{-1} region. Elemental analyses (C, H, N) were performed on an Elementar Vario EL III analytical instrument. UV-vis absorption spectra were recorded on a CARY 50 Probe spectrophotometer. Solution-state fluorescence spectra were obtained in oxygenated methanol solution at ambient temperature with a CARY Eclipse fluorescence spectrophotometer. Solid-state fluorescence spectra were recorded at ambient temperature on a Hitachi F4500 fluorescence spectrophotometer.

Synthesis of 4-(salicylideneimino)benzonitrile ($\text{Hsal}^{\text{H}}\text{-4-CN}$)

To a solution of 4-aminobenzonitrile (0.59 g, 5.0 mmol) in CH_3OH (10 mL) was added a solution of salicylaldehyde (0.52 mL, 5.0 mmol) in CH_3OH (5 mL) under nitrogen atmosphere. After the mixture was stirred for 4–5 h at room temperature, the solvent was removed under reduced pressure and the residue was washed with CH_3OH to give $\text{Hsal}^{\text{H}}\text{-4-CN}$ as a bright orange precipitate. Yield 48% (0.53 g, 2.4 mmol). ^1H NMR (300 MHz, $\text{DMSO-}d_6$, ppm): δ 12.42 (br, s, 1H), 8.96 (s, 1H), 7.92 (dd, $J = 6.6, 1.8$ Hz, 2H), 7.70 (dd, $J = 8.4, 1.8$ Hz, 1H), 7.55 (dd, $J = 6.6, 1.8$ Hz, 2H), 7.45 (td, $J = 7.8, 1.8$ Hz, 1H), 6.99 (t, $J = 7.8$ Hz, 1H), 6.98 (d, $J = 7.8$ Hz, 1H). MS (MALDI-TOF $^+$): m/z 222.915 [M] $^+$. IR (KBr pellet, cm^{-1}): 3060 (w), 2223 (m), 1614 (m), 1592 (s), 1561 (s), 1490 (s), 1451 (s), 1392 (w), 1358 (w), 1272 (s), 1190 (w), 1170 (m), 1150 (s), 1030 (w), 972 (w), 943 (w), 904 (w), 857 (s), 821 (s), 757 (s), 620 (w), 557 (m), 542 (m), 496 (w), 434 (m). Anal. calcd for $\text{C}_{14}\text{H}_{10}\text{N}_2\text{O}$: C, 75.66; H, 4.54; N, 12.60%. Found: C, 75.74; H, 4.52; N, 12.60%. Orange plate-shaped single crystals of $\text{Hsal}^{\text{H}}\text{-4-CN}$ suitable for X-ray diffraction were obtained by slow evaporation of the solvent from a dichloromethane solution at room temperature.

Synthesis of 4-(5'-chlorosalicylideneimino)benzonitrile ($\text{Hsal}^{\text{Cl}}\text{-4-CN}$)

This compound as an orange powder was prepared by a similar synthetic procedure to that for $\text{Hsal}^{\text{H}}\text{-4-CN}$. 4-Aminobenzonitrile (0.59 g, 5.0 mmol), 5-chlorosalicylaldehyde (0.78 g, 5.0 mmol). Yield 70% (0.91 g, 3.5 mmol). ^1H NMR (300 MHz, $\text{DMSO-}d_6$, ppm): δ 12.28 (br, s, 1H), 8.91 (s, 1H), 7.92 (dd, $J = 8.4, 1.2$ Hz, 2H), 7.78 (dd, $J = 2.7, 1.2$ Hz, 1H), 7.52 (dd, $J = 8.4, 1.2$ Hz, 2H), 7.47 (ddd, $J = 9.0, 3.0, 1.5$ Hz, 1H), 7.01 (dd, $J = 9.0, 1.2$ Hz, 1H). MS (MALDI-TOF $^+$): m/z 256.911 [M] $^+$. IR (KBr pellet, cm^{-1}): 3428 (s), 2224 (m), 1572 (s), 1474 (s), 1353 (m), 1283 (s), 1169 (s), 867 (w), 841 (m), 813 (s). Anal. calcd for $\text{C}_{14}\text{H}_9\text{ClN}_2\text{O}$: C, 65.51; H, 3.53; N, 10.91%. Found: C, 65.56; H, 3.61; N, 11.02%.

Synthesis of 4-(5'-bromosalicylideneimino)benzonitrile ($\text{Hsal}^{\text{Br}}\text{-4-CN}$)

This compound as an orange powder was prepared by a similar synthetic procedure to that for $\text{Hsal}^{\text{H}}\text{-4-CN}$. 4-Aminobenzonitrile (0.59 g, 5.0 mmol), 5-bromosalicylaldehyde (1.00 g, 5.0 mmol). Yield 82% (1.22 g, 4.1 mmol). ^1H NMR (300 MHz, $\text{DMSO-}d_6$, ppm): δ 12.30 (br, s, 1H), 8.90 (s, 1H), 7.93–7.89 (m, 3H), 7.58 (dd, $J = 8.7, 2.7$ Hz, 1H), 7.52 (dd, $J = 8.7, 1.8$ Hz, 2H), 6.96 (d, $J = 8.7$ Hz, 1H). MS (MALDI-TOF $^+$): m/z 300.922 [M] $^+$. IR (KBr pellet, cm^{-1}): 3747 (w), 3673 (w), 3060 (w), 2222 (m), 1619 (m), 1592 (s), 1557 (s), 1501 (m), 1472 (s), 1414 (w), 1356 (s), 1277 (s), 1224 (w), 1171 (s), 1122 (w), 1074 (w), 976 (w), 915 (w), 842 (m), 814 (s), 752 (w), 642 (w), 626 (w), 563 (w), 542 (m), 440 (w). Anal. calcd for $\text{C}_{14}\text{H}_9\text{BrN}_2\text{O}$: C, 55.84; H, 3.01; N, 9.30%. Found: C, 55.86; H, 3.02; N, 9.37%.

Synthesis of 4-(5'-methoxysalicylideneimino)benzonitrile ($\text{Hsal}^{\text{OMe}}\text{-4-CN}$)

This compound as a yellow powder was prepared by a similar synthetic procedure to that for $\text{Hsal}^{\text{H}}\text{-4-CN}$. 4-Aminobenzonitrile (0.59 g, 5.0 mmol), 5-methoxysalicylaldehyde (0.76 g, 5.0 mmol). Yield 74% (0.94 g, 3.7 mmol). ^1H NMR (300 MHz, $\text{DMSO-}d_6$, ppm): δ 11.75 (br, s, 1H), 8.91 (s, 1H), 7.91 (d, $J = 8.1$ Hz, 2H), 7.51 (d, $J = 8.1$ Hz, 2H), 7.28 (d, $J = 3.3$ Hz, 1H), 7.08 (ddd, $J = 9.0, 3.0, 0.6$ Hz, 1H), 6.92 (d, $J = 9.0$ Hz, 1H), 3.74 (d, $J = 0.6$ Hz, 3H). MS (MALDI-TOF $^+$): m/z 252.971 [M] $^+$. IR (KBr pellet, cm^{-1}): 2967 (w), 2839 (w), 2222 (m), 1616 (w), 1573 (s), 1489 (s), 1448 (w), 1387 (w), 1359 (w), 1314 (w), 1270 (s), 1215 (w), 1155 (s), 1037 (s), 986 (m), 939 (m), 874 (m), 842 (m), 771 (m), 715 (w), 650 (w), 557 (m), 485 (w), 441 (w). Anal. calcd for $\text{C}_{15}\text{H}_{12}\text{N}_2\text{O}_2$: C, 71.42; H, 4.79; N, 11.10%. Found: C, 71.29; H, 4.78; N, 11.16%. Orange plate-shaped single crystals of $\text{Hsal}^{\text{OMe}}\text{-4-CN}$ suitable for X-ray diffraction were obtained by slow evaporation of the solvent from a dichloromethane solution at room temperature.

Synthesis of $[\text{HNET}_3][\text{Zn}(\text{sal}^{\text{H}}\text{-4-CN})\text{Cl}_2]$ (**1**)

A solution of ZnCl_2 (136.3 mg, 1.0 mmol) in CH_3OH (7 mL) was added to a solution of $\text{Hsal}^{\text{H}}\text{-4-CN}$ (222.0 mg, 1.0 mmol)

in THF (7 mL) under nitrogen atmosphere, the mixture was stirred for 10 min. Then triethylamine (NEt₃, 99%, 16 drops) was added, and the mixture was stirred at room temperature overnight. The solvent was removed under reduced pressure and then ethyl ether was added. The resulting bright yellow precipitates were filtered. Yield 39% (180.0 mg, 3.9×10^{-1} mmol). ¹H NMR (300 MHz, DMSO-*d*₆, ppm): δ 8.59 (s, 1H), 7.96–7.90 (m, 2H), 7.78 (d, *J* = 8.4 Hz, 2H), 7.38 (d, *J* = 7.5 Hz, 1H), 7.30 (t, *J* = 7.2 Hz, 1H), 6.62 (d, *J* = 8.4 Hz, 1H), 6.53 (t, *J* = 7.2 Hz, 1H), 2.93 (q, *J* = 7.2 Hz, 6H), 1.10 (t, *J* = 7.2, Hz, 9H). IR (KBr pellet, cm⁻¹): 3502 (m), 2982 (w), 2942 (w), 2695 (w), 2227 (m), 1614 (m), 1599 (w), 1587 (s), 1538 (s), 1502 (w), 1468 (m), 1440 (s), 1395 (m), 1298 (m), 1255 (w), 1229 (w), 1171 (w), 1155 (m), 1063 (w), 1036 (w), 1017 (w), 994 (w), 926 (w), 862 (w), 842 (m), 810 (w), 790 (w), 766 (w), 758 (w), 744 (w), 586 (w), 554 (w), 503 (w), 474 (w), 462 (w). Anal. calcd for C₂₀H₂₅Cl₂N₃OZn·H₂O: C, 50.28; H, 5.70; N, 8.80%. Found: C, 50.06; H, 5.49; N, 8.99%. Yellowish-colored plate-shaped single crystals of **1** suitable for X-ray diffraction were obtained by slow evaporation of the solvent from a THF solution at room temperature.

Synthesis of [HNEt₃][Zn(sal^{Cl}-4-CN)Cl₂] (**2**)

Compound **2** as a yellow powder was prepared by a similar synthetic procedure to that for **1**. ZnCl₂ (280.0 mg, 2.1 mmol), Hsal^{Cl}-4-CN (510.0 mg, 2.0 mmol). Yield 85% (859.6 mg, 1.7 mmol). ¹H NMR (300 MHz, DMSO-*d*₆, ppm): δ 8.59 (s, 1H), 7.95 (d, *J* = 7.8 Hz, 2H), 7.78 (d, *J* = 7.5 Hz, 2H), 7.47 (d, *J* = 2.4 Hz, 1H), 7.27 (dd, *J* = 9.0, 2.4 Hz, 1H), 6.64 (d, *J* = 9.0 Hz, 1H), 2.97 (q, *J* = 7.2 Hz, 6H), 1.12 (t, *J* = 7.2 Hz, 9H). IR (KBr pellet, cm⁻¹): 3477 (m), 2976 (w), 2693 (m), 2500 (w), 2225 (m), 1613 (m), 1583 (s), 1525 (s), 1457 (s), 1426 (w), 1389 (s), 1301 (m), 1283 (m), 1153 (s), 1136 (m), 1013 (w), 872 (w), 837 (m), 822 (m), 760 (w), 679 (m), 559 (w), 540 (m), 491 (w), 459 (w). Anal. calcd for C₂₀H₂₄Cl₃N₃OZn·H₂O: C, 46.90; H, 5.12; N, 8.20%. Found: C, 46.55; H, 3.97; N, 7.89%. Orange-yellow single crystals of **2** suitable for X-ray diffraction were recrystallized in tetrahydrofuran–ethyl ether at room temperature.

Synthesis of [HNEt₃][Zn(sal^{Br}-4-CN)Cl₂] (**3**)

Compound **3** as a yellow powder was prepared by a similar synthetic procedure to that for **1**. ZnCl₂ (280.0 mg, 2.1 mmol), Hsal^{Br}-4-CN (602.2 mg, 2.0 mmol). Yield 85% (906.7 mg, 1.7 mmol). ¹H NMR (300 MHz, DMSO-*d*₆, ppm): δ 8.57 (s, 1H), 7.94 (d, *J* = 8.1 Hz, 2H), 7.78 (d, *J* = 7.8 Hz, 2H), 7.60 (d, *J* = 2.4 Hz, 1H), 7.36 (dd, *J* = 8.7, 2.4 Hz, 1H), 6.59 (d, *J* = 9.0 Hz, 1H), 2.97 (q, *J* = 7.2 Hz, 6H), 1.12 (t, *J* = 7.2 Hz, 9H). IR (KBr pellet, cm⁻¹): 3478 (s), 3192 (w), 3044 (w), 2980 (w), 2722 (m), 2221 (m), 1612 (m), 1596 (m), 1583 (s), 1520 (s), 1498 (m), 1458 (s), 1392 (s), 13115 (w), 1305 (w), 1158 (s), 1027 (w), 1000 (w), 930 (w), 895 (w), 870 (w), 849 (w), 825 (m), 796 (w), 656 (w), 645 (w), 557 (w), 542 (w), 495 (w), 460 (w). Anal. calcd for C₂₀H₂₄BrCl₂N₃OZn·H₂O: C, 43.15; H, 4.71; N, 7.55%. Found: C, 42.72; H, 4.80; N, 7.48%. Yellow-orange plate-shaped single crystals of **3** suitable for X-ray diffraction were recrystallized in tetrahydrofuran–ethyl ether at room temperature.

Synthesis of [HNEt₃][Zn(sal^{OMe}-4-CN)Cl₂] (**4**)

Compound **4** as an orange powder was prepared by a similar synthetic procedure to that for **1**. ZnCl₂ (130.0 mg, 9.5×10^{-1} mmol), Hsal^{OMe}-4-CN (250.0 g, 1.0 mmol). Yield 71% (328.5 mg, 6.7×10^{-1} mmol). ¹H NMR (300 MHz, DMSO-*d*₆, ppm): δ 8.59 (s, 1H), 7.93 (d, *J* = 8.1 Hz, 2H), 7.76 (d, *J* = 8.4 Hz, 2H), 7.01 (dd, *J* = 9.0, 3.0 Hz, 1H), 6.94 (d, *J* = 3.0 Hz, 1H), 6.59 (d, *J* = 8.7 Hz, 1H), 3.67 (s, 3H), 2.88 (q, br, *J* = 7.2 Hz, 6H), 1.08 (t, *J* = 7.2 Hz, 9H). IR (KBr pellet, cm⁻¹): 3475 (w), 2982 (w), 2661 (w), 2222 (m), 1586 (s), 1539 (s), 1474 (s), 1390 (m), 1356 (w), 1286 (m), 1222 (m), 1157 (s), 1037 (m), 888 (w), 843 (w), 806 (w), 720 (w), 553 (w), 495 (w), 459 (w). Anal. calcd for C₂₁H₂₇Cl₂N₃O₂Zn·H₂O: C, 49.67; H, 5.76; N, 8.28%. Found: C, 49.55; H, 4.44; N, 7.96%. Orange-colored block-shaped single crystals of **4** suitable for X-ray diffraction were recrystallized in dichloromethane–ethyl ether at room temperature.

Synthesis of [NEt₄][Zn(sal^H-4-CN)Cl₂] (**5**)

To a solution of **1** (247.5 mg, 0.5 mmol) in THF (6 mL) was added a solution of NEt₄Cl (83.0 mg, 0.5 mmol) in CH₃OH (10 mL). The mixture was stirred at room temperature for several hours and then the resulting yellow precipitates were filtered. Yield 42% (103.5 mg, 2.1×10^{-1} mmol). ¹H NMR (300 MHz, DMSO-*d*₆, ppm): δ 8.58 (s, 1H), 7.94 (d, *J* = 8.7 Hz, 2H), 7.80 (d, *J* = 8.4 Hz, 2H), 7.40–7.27 (m, 2H), 6.62 (d, *J* = 8.7 Hz, 1H), 6.53 (t, *J* = 7.5 Hz, 1H), 3.20 (q, *J* = 7.2 Hz, 8H), 1.16 (tt, *J* = 7.2, 1.8 Hz, 12H). IR (KBr pellet, cm⁻¹): ν 3055 (w), 2980 (w), 2949 (w), 2229 (m), 1614 (m), 1597 (m), 1584 (s), 1531 (s), 1506 (w), 1459 (s), 1438 (s), 1395 (s), 1349 (w), 1328 (w), 1309 (w), 1170 (s), 1147 (s), 1127 (w), 1082 (w), 1030 (w), 1003 (w), 990 (w), 925 (w), 862 (w), 841 (m), 803 (w), 790 (w), 765 (m), 620 (w), 590 (m), 553 (m), 545 (m). Anal. calcd for C₂₂H₂₆Cl₂N₃OZn: C, 54.17; H, 5.99; N, 8.61%. Found: C, 53.98; H, 5.98; N, 8.66%. Bright-yellow plate-shaped single crystals of **5** suitable for X-ray diffraction were recrystallized in dichloromethane–ethyl ether at room temperature.

X-Ray crystallographic analyses

Single-crystal X-ray diffraction analysis was performed by using a Bruker Smart CCD diffractometer equipped with graphite monochromatized Mo Kα radiation ($\lambda = 0.71073$ Å). Starting models for structure refinement were found using direct methods (SHELXS-97²⁰ for Hsal^H-4-CN, **1–4**, and **5**, and SIR92²¹ for Hsal^{OMe}-4-CN), and the structural data were refined by full-matrix least-squares methods on *F*² using the WINGX²² and SHELX-97²⁰ program packages. Anisotropic thermal factors were assigned to non-hydrogen atoms. Carbon-bound hydrogen atoms were placed in calculated positions with isotropic displacement parameters. Oxygen- and nitrogen-bound hydrogen atoms were structurally evident in difference Fourier maps and refined isotropically in the riding-model approximation with bond length and angles restraints. Experimental details for X-ray data collection and the refinements are summarized in Table 1. CCDC 935863–935869 contain the supplementary crystallographic data for this paper.

Table 1 Crystallographic data for Hsal^H-4-CN, Hsal^{OMe}-4-CN, and zinc-salicylideneimine compounds 1–5

	Hsal ^H -4-CN	Hsal ^{OMe} -4-CN	1	2
Empirical formula	C ₁₄ H ₁₀ N ₂ O	C ₁₅ H ₁₂ N ₂ O ₂	C ₂₀ H ₂₅ Cl ₂ N ₃ OZn	C ₂₀ H ₂₄ Cl ₃ N ₃ OZn
<i>M_w</i>	222.24	252.27	459.70	494.14
Crystal system	Monoclinic	Orthorhombic	Monoclinic	Monoclinic
Space group	<i>C2/c</i>	<i>Pbca</i>	<i>P2₁/c</i>	<i>P2₁/n</i>
<i>a</i> /Å	28.075(6)	13.2684(16)	7.1423(2)	7.7224(4)
<i>b</i> /Å	5.7634(12)	6.2747(6)	13.0443(5)	12.2159(6)
<i>c</i> /Å	14.427(3)	29.454(4)	23.0388(8)	23.6010(11)
β /°	97.497(8)	90	94.2670(10)	95.2300(10)
<i>V</i> /Å ³	2192.4(8)	2452.2(5)	2140.49(13)	2217.16(19)
<i>Z</i>	8	8	4	4
<i>T</i> /K	296(2)	296(2)	296(2)	298(2)
λ /Å	0.71073	0.71073	0.71073	0.71073
<i>D</i> _{calc} /g cm ⁻³	1.347	1.367	1.426	1.480
<i>F</i> ₀₀₀	928	1056	952	1016
μ /mm ⁻¹	0.087	0.093	1.411	1.485
θ _{min} , θ _{max} /°	2.87, 25.01	2.07, 25.07	1.77, 24.85	1.88, 26.02
Refl. collected	7165	8020	13 248	12 175
Unique refl. (<i>R</i> _{int})	1911 (0.0324)	2124 (0.0557)	3687 (0.0177)	4368 (0.0220)
Obs. refl. (<i>I</i> > 2 σ (<i>I</i>))	1462	1413	3391	3882
Parameters	157	173	247	256
<i>R</i> ₁ ^a (<i>I</i> > 2 σ (<i>I</i>))	0.0365	0.0435	0.0197	0.0255
<i>wR</i> ₂ ^b (<i>I</i> > 2 σ (<i>I</i>))	0.0848	0.1061	0.0512	0.0664
<i>R</i> ₁ ^a (all data)	0.0541	0.0745	0.0224	0.0299
<i>wR</i> ₂ ^b (all data)	0.0934	0.1230	0.0526	0.0686
GOF on <i>F</i> ²	1.039	1.010	1.069	1.045
$\Delta\rho$ _{max} / $\Delta\rho$ _{min} (e Å ⁻³)	0.190/−0.215	0.188/−0.198	0.303/−0.223	0.369/−0.238
	3	4	5	
Empirical formula	C ₂₀ H ₂₄ BrCl ₂ N ₃ OZn	C ₂₁ H ₂₇ Cl ₂ N ₃ O ₂ Zn	C ₂₂ H ₂₉ Cl ₂ N ₃ OZn	
<i>M_w</i>	538.60	489.73	487.75	
Crystal system	Monoclinic	Monoclinic	Monoclinic	
Space group	<i>P2₁/n</i>	<i>C2/c</i>	<i>P2₁/n</i>	
<i>a</i> /Å	7.786(2)	46.477(5)	13.1246(7)	
<i>b</i> /Å	12.174(3)	7.1762(9)	10.1242(6)	
<i>c</i> /Å	23.664(6)	27.535(3)	18.2879(10)	
β /°	95.371(11)	91.359(4)	109.496(2)	
<i>V</i> /Å ³	2233.3(10)	9181.1(18)	2290.7(2)	
<i>Z</i>	4	16	4	
<i>T</i> /K	296(2)	200(2)	200(2)	
λ /Å	0.71073	0.71073	0.71073	
<i>D</i> _{calc} /g cm ⁻³	1.602	1.417	1.414	
<i>F</i> ₀₀₀	1088	4064	1016	
μ /mm ⁻¹	3.144	1.324	1.323	
θ _{min} , θ _{max} /°	1.73, 25.07	0.88, 24.95	2.32, 25.02	
Refl. collected	14 686	25 087	14 577	
Unique refl. (<i>R</i> _{int})	3935 (0.0184)	8032 (0.1995)	4010 (0.0274)	
Obs. refl. (<i>I</i> > 2 σ (<i>I</i>))	3377	3208	3382	
Parameters	256	531	262	
<i>R</i> ₁ ^a (<i>I</i> > 2 σ (<i>I</i>))	0.0242	0.0702	0.0283	
<i>wR</i> ₂ ^b (<i>I</i> > 2 σ (<i>I</i>))	0.0540	0.0783	0.0769	
<i>R</i> ₁ ^a (all data)	0.0314	0.2114	0.0386	
<i>wR</i> ₂ ^b (all data)	0.0563	0.1084	0.0900	
GOF on <i>F</i> ²	1.045	0.910	1.134	
$\Delta\rho$ _{max} / $\Delta\rho$ _{min} (e Å ⁻³)	0.283/−0.326	0.464/−0.547	0.347/−0.344	

$$^a R_1 = \sum ||F_o| - |F_c|| / \sum |F_o|, \quad ^b wR_2 = \{ \sum [w(F_o^2 - F_c^2)^2] / \sum [w(F_o^2)^2] \}^{1/2}.$$

Results and discussion

Synthesis and characterization of salicylideneimine ligands

The four cyano-functionalized salicylideneimine ligands, abbreviated as Hsal^H-4-CN, Hsal^{Cl}-4-CN, Hsal^{Br}-4-CN, and Hsal^{OMe}-4-CN, are synthesized by the condensation reactions of 4-aminobenzonitrile and corresponding salicylaldehydes with a 1:1 molar ratio in methanol at room temperature.

Their molecular structures are characterized by ¹H NMR (Fig. S1–S4, ESI[†]) and mass spectra unambiguously. These ligands are soluble in a range of organic solvents and are stable to hydrolysis and to aerial oxidation both in the solid-state and in solution over several weeks. The solid-state structures of Hsal^H-4-CN and Hsal^{OMe}-4-CN are further determined by single-crystal X-ray diffraction analysis (Fig. 1). There is a strong intramolecular O–H...N hydrogen bond, with the O...N

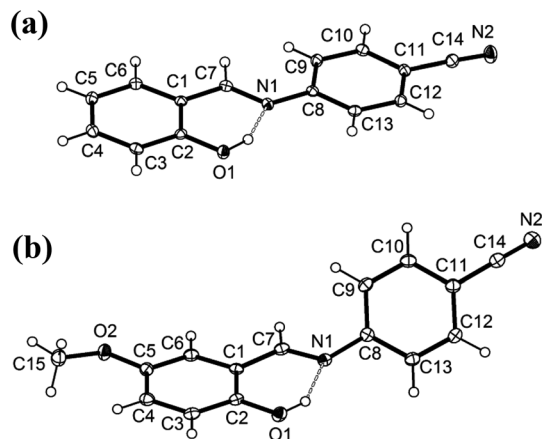


Fig. 1 Molecular structures and atomic numbering schemes of salicylideneimine ligands: (a) Hsal^H-4-CN and (b) Hsal^{OMe}-4-CN. Displacement ellipsoids are drawn at the 30% probability level.

Table 2 Hydrogen bonding parameters for salicylideneimine ligands Hsal^H-4-CN and Hsal^{OMe}-4-CN and zinc-salicylideneimine compounds **1–4**

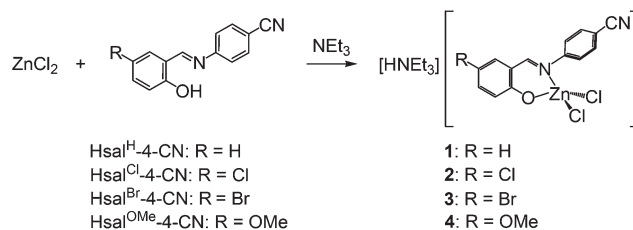
D–H...A	D–H (Å)	H...A (Å)	D...A (Å)	D–H...A (°)
Hsal ^H -4-CN				
O1–H101...N1	0.94	1.74	2.6119(17)	152
Hsal ^{OMe} -4-CN				
O1–H101...N1	0.90	1.83	2.6288(18)	146
1				
N3–H101...O1	0.87	1.98	2.8275(16)	166
2				
N3–H101...O1	0.90	1.94	2.8253(19)	171
3				
N3–H101...O1	0.99	1.85	2.812(2)	166
4				
N3–H101...O1	0.87	1.92	2.773(7)	166
N6–H102...O3	0.87	1.94	2.793(8)	168

distance of 2.6119(17) Å for Hsal-4-CN and 2.6288(18) Å for Hsal^{OMe}-4-CN (Table 2), between the phenol hydrogen and the azomethine nitrogen for each of the two structures. In addition, the benzonitrile phenyl ring and the salicylideneimine phenyl ring twist from each other, with a dihedral angle of 3.3° for Hsal^H-4-CN and 41.9° for Hsal^{OMe}-4-CN.

Synthesis and crystal structure of zinc-salicylideneimine compounds

Ionic zinc-salicylideneimine compounds with a general formula [HNEt₃][Zn(L)Cl₂] (L = sal^H-4-CN, **1**; sal^{Cl}-4-CN, **2**; sal^{Br}-4-CN, **3**; sal^{OMe}-4-CN, **4**) are synthesized in moderate to high yields from the complexation reactions of ZnCl₂ and corresponding salicylideneimine ligands with a 1:1 stoichiometry of zinc to ligand in the presence of several drops of triethylamine (NEt₃) in a refluxing THF-methanol solution (Scheme 1). Their molecular structures are characterized by ¹H NMR spectra (see below for detailed discussion) and single-crystal X-ray diffraction analyses.

Solid-state structure analyses confirm that **1–4** have similar crystal structures, as shown in Fig. 2, consisting of a



Scheme 1 Syntheses of zinc-salicylideneimine compounds **1–4**.

triethylammonium cation, HNEt₃⁺, and an anionic Zn-salicylideneimine counterpart, [Zn(L)Cl₂][−]. The HNEt₃⁺ cationic part and the [Zn(L)Cl₂][−] anionic part attract each other through not only electrostatic force, but also an N–H...O hydrogen-bonding interaction between the triethylammonium proton and the phenolato oxygen ($d(\text{N}\cdots\text{O}) = 2.773(7)\text{--}2.8275(16)$ Å, Table 2). Within the [Zn(L)Cl₂][−] anionic part, the Zn center is chelated by one azomethine and one phenolato groups from one salicylideneimine ligand and coordinated by two chloro ligands, giving rise to a distorted tetrahedral geometry. For **1**, the Zn–O bond length of 1.9598(11) Å and the Zn–N bond length of 2.0471(13) Å are normal, as well as the Zn–Cl bond length of 2.2300(4) and 2.2452(4) Å (Table S1[†]). The O–Zn–N bite angle for the chelating sal^H-4-CN ligand is 94.00(5)°. The benzonitrile phenyl ring twists from the salicylideneimine phenyl ring with a dihedral angle of 26.5°. For **2–4**, the metric data are similar to those for **1**, except that the dihedral angle between the benzonitrile phenyl ring and the salicylideneimine phenyl ring spans over a wide range, from 1.9 to 36.5° (Table S1[†]).

¹H NMR studies

¹H NMR spectrum of **1** in deuterated dimethylsulfoxide (DMSO-*d*₆) solvent, recorded at the concentration of $\approx 2.0 \times 10^{-2}$ M, is of particular notice and shows two different sets of remarkably sharp signals in the aromatic region and only one set of slightly broadened signals in the aliphatic region (Fig. 3 and S5c[†]). These complicated resonances in the aromatic region are reasonably attributed to two different materials having aromatic hydrogens. The first set of signals showing the azomethine proton (CH=N) resonance at δ 8.96 ppm and the phenol proton resonance at δ 12.37 ppm exhibits almost identical ¹H NMR signals, in terms of peak position and shape, as those recorded for free Hsal^H-4-CN ligand in DMSO-*d*₆ solvent, with the azomethine and the phenol protons at δ 8.96 and 12.42 ppm, respectively. The second set of signals having a relative upfield position of δ 8.58 ppm for the azomethine proton resonance is assigned to the anionic counterpart, [Zn(sal^H-4-CN)Cl₂][−], of **1**. Furthermore, the triethylammonium (HNEt₃⁺) cation of **1** shows resonances at δ 2.93 and 1.10 ppm with the expected multiplicity, according to its molecular structure, for the methylene (HN(CH₂CH₃)₃⁺) and methyl (HN(CH₂CH₃)₃⁺) protons, respectively. In addition, it is of particular surprise that in the aromatic region the signals from the free Hsal^H-4-CN ligand are always observed in the ¹H NMR spectra of **1** in several independent ¹H NMR

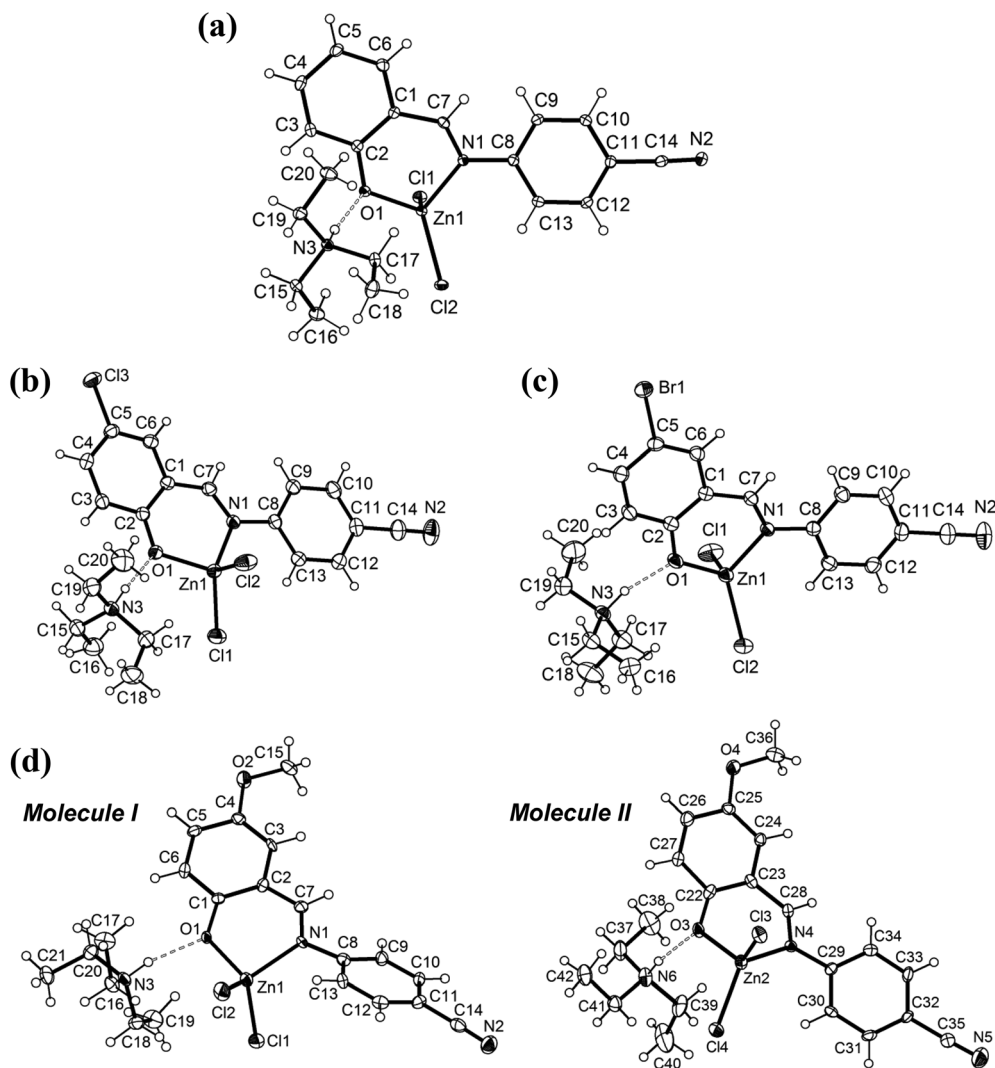


Fig. 2 Molecular structures and atomic numbering schemes of zinc-salicylideneimine compounds: (a) $[\text{HNEt}_3][\text{Zn}(\text{sal}^{\text{H}}\text{-4-CN})\text{Cl}_2]$ (**1**), (b) $[\text{HNEt}_3][\text{Zn}(\text{sal}^{\text{Cl}}\text{-4-CN})\text{Cl}_2]$ (**2**), (c) $[\text{HNEt}_3][\text{Zn}(\text{sal}^{\text{Br}}\text{-4-CN})\text{Cl}_2]$ (**3**), and (d) $[\text{HNEt}_3][\text{Zn}(\text{sal}^{\text{OMe}}\text{-4-CN})\text{Cl}_2]$ (**4**) (two crystallographically distinct molecules). Empty dashed lines represent the N-H...O hydrogen bonds. Displacement ellipsoids are drawn at the 30% probability level.

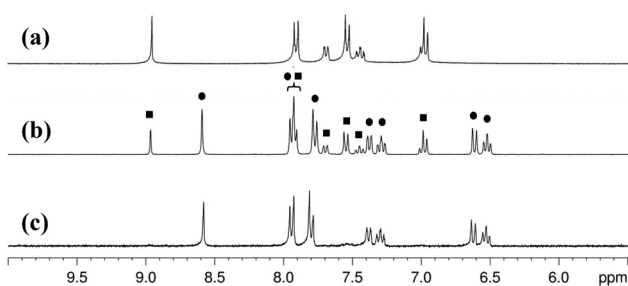


Fig. 3 Comparison of the aromatic region ^1H NMR spectra of (a) $\text{Hsal}^{\text{H}}\text{-4-CN}$, (b) $[\text{HNEt}_3][\text{Zn}(\text{sal}^{\text{H}}\text{-4-CN})\text{Cl}_2]$ (**1**), and (c) $[\text{NEt}_4][\text{Zn}(\text{sal}^{\text{H}}\text{-4-CN})\text{Cl}_2]$ (**5**) in $\text{DMSO-}d_6$ at room temperature. In (b), solid squares (■) and solid circles (●) represent the two sets of resonances assigning to the free form of $\text{Hsal}^{\text{H}}\text{-4-CN}$ ligand and the anionic complex part, $[\text{Zn}(\text{sal}^{\text{H}}\text{-4-CN})\text{Cl}_2]^-$, of **1**, respectively.

measurements ($\approx 2.0 \times 10^{-2}$ M), even dissolving the crystalline samples, with a particular ratio of approximately 1:2 in relative integrated area to the resonances from the $[\text{Zn}(\text{sal}^{\text{H}}\text{-4-CN})\text{Cl}_2]^-$ anion in **1**. These observations suggest that compound **1** would undergo ligand dissociation to give the neutral form of free $\text{Hsal}^{\text{H}}\text{-4-CN}$ ligand together with an un-identified zinc-based species. However, the simultaneous presence of both the complexed zinc-salicylideneimine species (complex $[\text{Zn}(\text{L})\text{Cl}_2]^-$ form) and the free salicylideneimine ligand (free ligand HL form) in solution can be rationalized in terms of a dynamic equilibrium of ligand dissociation and recoordination. In other words, there must be a forward process, *i.e.*, ligand dissociation, and a reverse process, *i.e.*, ligand recoordination, to complete such a dynamic equilibrium based on the results observed in the ^1H NMR studies. This reversible process can probably be achieved through shuttling protons between the phenolate and triethylammonium groups.

Zinc-salicylideneimine compounds **2-4**, with a chloro-, a bromo-, and a methoxy-substitution of the salicylidene ring, have also exhibited similar ^1H NMR spectra in $\text{DMSO-}d_6$ solvent ($\approx 2.0 \times 10^{-2}$ M) to that of **1** (Fig. S6c-S8c†), implying

measurements ($\approx 2.0 \times 10^{-2}$ M), even dissolving the crystalline samples, with a particular ratio of approximately 1:2 in relative integrated area to the resonances from the $[\text{Zn}(\text{sal}^{\text{H}}\text{-4-CN})\text{Cl}_2]^-$ anion in **1**. These observations suggest that compound **1** would undergo ligand dissociation to give the neutral form of free $\text{Hsal}^{\text{H}}\text{-4-CN}$ ligand together with an un-identified zinc-based species. However, the simultaneous presence of both the complexed zinc-salicylideneimine species (complex $[\text{Zn}(\text{L})\text{Cl}_2]^-$ form) and the free salicylideneimine ligand (free ligand HL form) in solution can be rationalized in terms of a dynamic equilibrium of ligand dissociation and recoordination. In other words, there must be a forward process, *i.e.*, ligand dissociation, and a reverse process, *i.e.*, ligand recoordination, to complete such a dynamic equilibrium based on the results observed in the ^1H NMR studies. This reversible process can probably be achieved through shuttling protons between the phenolate and triethylammonium groups.

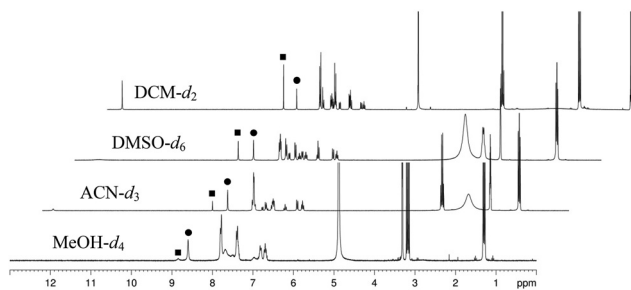


Fig. 4 ^1H NMR spectra of $[\text{HNET}_3][\text{Zn}(\text{sal}^{\text{H}}\text{-4-CN})\text{Cl}_2]$ (**1**) ($\approx 2.0 \times 10^{-2}$ M) in various solvents at room temperature. ■: azomethine proton ($\text{CH}=\text{N}$) in free form of $\text{Hsal}^{\text{H}}\text{-4-CN}$ ligand. ●: azomethine proton in complex form of $[\text{HNET}_3][\text{Zn}(\text{sal}^{\text{H}}\text{-4-CN})\text{Cl}_2]$ (**1**).

Table 3 Dissociation ratio (R_{D}) of zinc-salicylideneimine compounds **1–4** in various solvents at room temperature^a

	MeOH- d_4	ACN- d_3	DMSO- d_6	DCM- d_2
1	13.8	21.3	41.5	62.5
2	~0	2.9	21.3	42.9
3	~0	2.9	13.8	55.4
4	21.3	7.4	44.8	70.3

^a All the samples were prepared at 2.0×10^{-2} mol L⁻¹.

clearly the occurrence of a similar ligand dissociation/recoordination equilibrium for **2–4** in solution. However, in an effort to investigate the influence of solvent on the dissociation/recoordination properties of **1–4**, their ^1H NMR spectra are recorded in a series of further deuterated solvents including methanol- d_4 (MeOH- d_4), acetonitrile- d_3 (ACN- d_3), and dichloromethane- d_2 (DCM- d_2) at the concentration of $\approx 2.0 \times 10^{-2}$ M (Fig. 4 and S5–S8†). To illustrate the degree of ligand dissociation within **1–4** in solution of chosen deuterated solvents, the dissociation ratio (R_{D}) parameter is herein applied:

$$R_{\text{D}} = \frac{I_{\text{CH}=\text{N}}(\text{HL})}{I_{\text{CH}=\text{N}}(\text{HL}) + I_{\text{CH}=\text{N}}([\text{Zn}(\text{L})\text{Cl}_2]^-)} \times 100$$

where $I_{\text{CH}=\text{N}}(\text{HL})$ = relative integrated area of the azomethine proton ($\text{CH}=\text{N}$) signal of free ligand form and $I_{\text{CH}=\text{N}}([\text{Zn}(\text{L})\text{Cl}_2]^-)$ = relative integrated area of the azomethine proton ($\text{CH}=\text{N}$) signal of complex form. Table 3 summarizes the analyses of dissociation ratios for **1–4** in various solvents.

In general, solvent effects are described in terms of solvent strength/polarity, protic/aprotic characteristic, and/or coordination ability. When dissolved in noncoordinating, less polar aprotic DCM- d_2 (polarity index (P_{i}) = 3.1)²³ solvent, the greatest degree of ligand dissociation is observed for each of the zinc-salicylideneimine compounds (R_{D} = 61.7 for **1**, 42.9 for **2**, 55.4 for **3**, and 70.3 for **4**), which is approximately 2 to 4 times larger than the next largest R_{D} value in a solution of DMSO- d_6 (P_{i} = 7.2), a coordinating, high polar aprotic solvent. The lowest R_{D} value is observed in solutions of coordinating, moderately polar protic MeOH- d_4 (P_{i} = 5.1) and aprotic ACN- d_3 (P_{i} = 5.8) solvents for **1–3** and **4**, respectively.

According to the ^1H NMR studies, the dissociation/recoordination properties of **1–4** are dependent on not only the solvents but also the substitutions of the salicylidene ring. Indeed, substitution of chloro, bromo, and methoxy groups in place of hydrogen on the 5'-position of the salicylideneimine moiety within the structures of zinc-salicylideneimine compounds does have an impact on ligand dissociation/recoordination in solution. In a general view, compounds **2** and **3**, with 5-chloro and 5-bromo substitutions of the salicylidene ring, respectively, have the smallest degree of ligand dissociation, even near nondissociation ($R_{\text{D}} \sim 0$), in each of the chosen solvents, whilst compound **4**, with 5-methoxy substitution of the salicylidene ring, gives the largest R_{D} values in each of cases. This can reasonably be attributed to the inductive effects of their electronic features. Chloro- and bromo-substitution in the salicylidene fragment are electron-withdrawing groups that draw electrons toward themselves; thereby, the phenolato group has a less negative charge and, as a result, its lone pair less readily donates to the triethylammonium proton. Such a mechanism induces a smaller degree of ligand dissociation in comparison with other compounds in the same media. In contrast, the electron-donating methoxy substitution in the salicylidene fragment contributes electrons to the phenolato group, increasing its negative character and making it a stronger base to compete for the proton of the triethylammonium group. As a result, this demonstrates a relatively high tendency for ligand dissociation. Consequently, influences by both solvent and substitution effects give the scrambled order of ligand dissociation/recoordination of **1–4**. The R_{D} values are given in a trend in solvents as DCM- d_2 > DMSO- d_6 > ACN- d_3 > MeOH- d_4 for **1** and DCM- d_2 > DMSO- d_6 > MeOH- d_4 > ACN- d_3 for **4** as well as roughly DCM- d_2 > DMSO- d_6 > ACN- d_3 ~ MeOH- d_4 for **2** and **3**.

Additionally, the influence of concentration on the dissociation/recoordination properties of **1** has also been explored in DMSO- d_6 solvent at the concentrations of 4.0×10^{-3} – 1.0×10^{-1} M. As shown in Fig. 5, ^1H NMR signals of **1** in DMSO- d_6 solvent is indeed concentration dependent. Analyzing these ^1H NMR spectra reveals that with the decrease of the concentration of **1** the integration of the azomethine proton ($\text{CH}=\text{N}$) of the free $\text{Hsal}^{\text{H}}\text{-4-CN}$ ligand form increases, with that of the complex $[\text{Zn}(\text{L})\text{Cl}_2]^-$ form remaining almost constant. Herein the aspect of dissociation ratio is applied again for the purpose of understanding the relationship with the concentration of **1** in DMSO- d_6 , and the relevant data are summarized in Table S2† and reported in Fig. 6. Of particular interest, the dissociation ratios are nearly linearly related to the concentrations of **1** in two different slopes, with the existence of a turn at the concentration of 2.0×10^{-2} M. However, the negative slope implies that with the increase in the concentration, there is a decrease in the dissociation ratio. At concentrations higher than 2.0×10^{-2} M, ligand dissociation is mild with a smooth slope of the dissociation ratio against the concentration of **1**. On going to lower concentrations, $\leq 2.0 \times 10^{-2}$ M, compound **1** has more of a tendency toward ligand dissociation due to the observation of the steep slope. As a result,

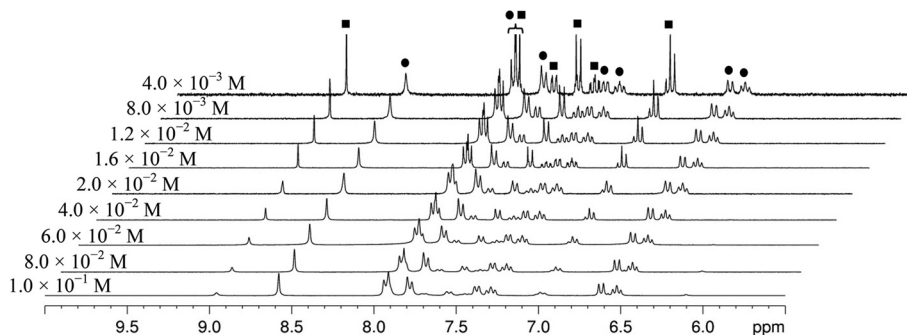


Fig. 5 Evolution of concentration-dependent ^1H NMR spectra of $[\text{HNEt}_3][\text{Zn}(\text{sal}^{\text{H}}\text{-4-CN})\text{Cl}_2]$ (**1**) in $\text{DMSO-}d_6$ at room temperature. Solid squares (\blacksquare) and solid circles (\bullet) represent the two sets of resonances assigning to the free form of $\text{Hsal}^{\text{H}}\text{-4-CN}$ ligand and the anionic complex part, $[\text{Zn}(\text{sal}^{\text{H}}\text{-4-CN})\text{Cl}_2]^-$, of **1**, respectively.

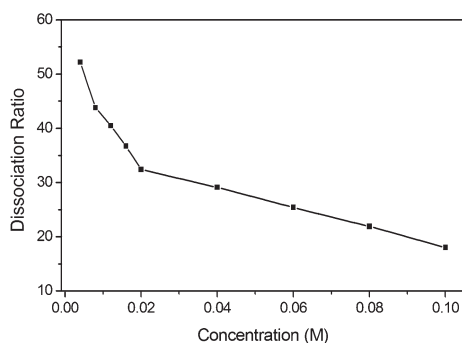


Fig. 6 Plot of the dissociation ratio against concentration of **1** in $\text{DMSO-}d_6$ at room temperature.

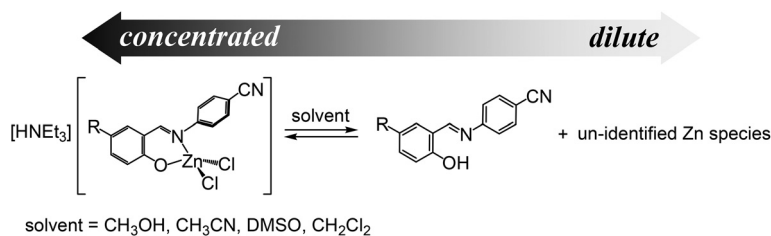
dilute solutions are likely characterized by the high degree of ligand dissociation, leading to the ratio being shifted toward the formation of the free ligand HL form, whereas at higher concentration, the equilibrium shifted in favor of the complex $[\text{Zn}(\text{L})\text{Cl}_2]^-$ form (Scheme 2), meaning that the ionic compound could be reformed from the dissociated species.

Photophysical properties

The photophysical properties (electronic absorption spectra and luminescence spectra) of salicylideneimine ligands $\text{Hsal}^{\text{R}}\text{-4-CN}$ ($\text{R} = \text{H}, \text{Cl}, \text{Br}, \text{and OMe}$) and the related ionic zinc-salicylideneimine compounds **1-4** have been studied in a range of solvents ($\text{DMSO}, \text{ACN}, \text{MeOH}, \text{DCM}$) at room temperature. The relevant absorption and emission parameters of all of the investigated compounds are collected in Table 4.

The electronic absorption spectra of $\text{Hsal}^{\text{R}}\text{-4-CN}$ ($\text{R} = \text{H}, \text{Cl}, \text{Br}, \text{and OMe}$) ligands in various solvents all display two intense absorption bands centered at around 280 and 350 nm ($\epsilon \sim 0.48\text{--}1.70 \times 10^4 \text{ M}^{-1} \text{ cm}^{-1}$) (Fig. S10 \dagger), presumably involving $\pi \rightarrow \pi^*$ and $n \rightarrow \pi^*$ transitions, respectively.^{16c,24-31} Compounds **1-4**, as shown in Fig. 7, exhibit intense transitions in the UV region, which correspond to intraligand (IL) charge transfer transitions, along with a new, moderately intense feature ($\epsilon \sim 1.8\text{--}8.3 \times 10^3 \text{ M}^{-1} \text{ cm}^{-1}$) between 390 and 460 nm, absent in the absorption spectrum of the free ligand. The longer wavelength transition may be assigned to a metal-to-ligand charge transfer (MLCT) transition involving the $d^{10}(\text{Zn}) \rightarrow \pi^*(\text{azomethine})$ character.²⁵ However, the complexes do not exhibit any significant solvatochromism. In addition, it is also observed that the electron-donating methoxy substitution of the salicylidene ring in $\text{Hsal}^{\text{OMe}}\text{-4-CN}$ and compound **4** causes bathochromic shift on absorption bands relative to that of the unsubstituted $\text{Hsal}^{\text{H}}\text{-4-CN}$ and compound **1**, respectively.

Fluorescence studies of **1-4**, in the same range of solvents, all indicate a noticeably unstructured band with a maximum between 515–560 nm, independent of the excitation wavelength (Fig. 8). In comparison, the related salicylideneimine ligands are considered to be fluorescence silent even though there are very weak, negligible broadened emission bands ($\lambda_{\text{max}} = \sim 520\text{--}561 \text{ nm}$) for the ligands in solvents (Fig. S11 \dagger). The fluorescence of the free ligands may be quenched by the occurrence of a photoinduced electron transfer (PET) mechanism, in which electrons are induced by the exciting radiation to transfer from the lone pair of azomethine N-donor to the π -system of the fluorophore and in so doing quench the



Scheme 2 Concentration-dependent ligand dissociation/recoordination equilibrium.

Table 4 Photophysical data for salicylideneimine ligands and zinc–salicylideneimine compounds in various solvents (1.0×10^{-4} M) and in solid-state at room temperature

Compound	Medium	Absorption $\lambda_{\text{max}}/\text{nm}$ ($\epsilon/\text{M}^{-1} \text{cm}^{-1}$)	Fluorescence $\lambda_{\text{max}}/\text{nm}$ ($\lambda_{\text{ex}}/\text{nm}$)
Hsal ^H -4-CN	MeOH	285 (15 700), 340 (11 500)	~539 (350)
	ACN	280 (14 900), 340 (11 800)	~520 (400)
	DMSO	285 (17 000), 345 (15 700)	~540 (325)
	DCM	280 (16 600), 340 (11 600)	~544 (350)
	Solid-state	—	569 (350)
Hsal ^{Cl} -4-CN	MeOH	280 (16 400), 355 (8300)	~539 (350)
	ACN	280 (14 300), 355 (10 100)	~545 (350)
	DMSO	290 (10 700), 355 (9300)	~543 (300)
	DCM	280 (14 800), 360 (10 700)	~549 (350)
	Solid-state	—	574 (430)
Hsal ^{Br} -4-CN	MeOH	280 (15 200), 355 (7600)	~546 (350)
	ACN	280 (15 800), 355 (10 900)	~546 (350)
	DMSO	285 (11 700), 355 (9600)	~546 (300)
	DCM	280 (14 400), 360 (9800)	~546 (350)
	Solid-state	—	569 (360)
Hsal ^{OMe} -4-CN	MeOH	290 (13 700), 375 (6700)	~554 (325)
	ACN	290 (14 300), 375 (7900)	~561 (350)
	DMSO	290 (7300), 380 (4800)	~560 (325)
	DCM	295 (13 300), 380 (7800)	~558 (350)
	Solid-state	—	623 (400)
1	MeOH	295 (12 000), 355 (5400), 390 (4600)	515 (325)
	ACN	295 (12 900), 410 (8300)	520 (315)
	DMSO	285 (11 200), 345 (8000), 415 (1800)	519 (315)
	DCM	285 (14 600), 345 (9200), 420sh	515 (310)
	Solid-state	—	529 (350)
2	MeOH	285 (9700), 365 (3600), 405 (3400)	522 (325)
	ACN	295 (9600), 420 (6500)	525 (310)
	DMSO	280 (8600), 360 (5800), 420 (2100)	528 (320)
	DCM	290 (12 500), 365 (5900), 420 (4900)	528 (315)
	Solid-state	—	542 (480)
3	MeOH	290 (10 700), 365 (3800), 400 (4000)	521 (315)
	ACN	290 (11 600), 420 (7700)	525 (320)
	DMSO	290 (11 200), 360 (7200), 420 (2800)	528 (320)
	DCM	295 (11 500), 365 (5000), 420 (4500)	525 (320)
	Solid-state	—	544 (480)
4	MeOH	300 (12 500), 385 (4500), 400 (3300)	555 (325)
	ACN	300 (12 800), 385sh, 450 (6600)	560 (325)
	DMSO	290 (12 600), 380 (7500), 460sh	560 (325)
	DCM	295 (15 000), 385 (7200), 443sh	560 (325)
	Solid-state	—	573 (500)
5	MeOH	295 (13 400), 395 (5700)	516 (315)
	ACN	295 (15 100), 410 (10 600)	520 (325)
	DMSO	300 (14 400), 415 (9900)	519 (320)
	DCM	300 (13 700), 415 (8800)	518 (325)
	Solid-state	—	531 (350)

fluorescence.^{25,28,32,33} Therefore, high fluorescence behavior of **1–4** is reasonably attributed to the complex formation *via* the chelation of the salicylideneimine ligand to Zn(II) ion through the azomethine and phenolato groups; this effectively lessens the PET quenching effect and leads to the chelation enhanced fluorescence (CHEF) effect.^{25,28,33} The six-membered chelate ring present in the zinc–salicylideneimine complexes increases in rigidity in comparison to salicylideneimine ligands, which in turn, reduces the loss of energy by vibrational decay and enhances the fluorescent intensity.^{16c,25,28,33} For the Zn(II) complexes, emissions originating from metal-centered or MLCT/LMCT excited state are not encouraged since the Zn(II) ion has a stable d^{10} configuration that makes it difficult to oxidize or reduce. Thus, the emission observed in **1–4** is tentatively assigned to the intraligand ($\pi \rightarrow \pi^*$) fluorescence.^{25,34} In

the solid phase, compounds **1–4** all show very intense fluorescence with a maximum between 529–573 nm (Fig. S13[†]), which are red-shifted by 9–23 nm from the emission in solution phases at room temperature. This is probably caused by intermolecular interactions in the solid-phase that effectively lessen the energy gap.²⁵ Moreover, with an electron-donating methoxy group added on the salicyaldimine moiety, the emission bands in both solution- and solid-phase for **4** are observed to red shift (>40 nm) in comparison with these in **1**.

According to the results of the aforementioned ¹H NMR studies, compounds **1–4** exhibit an interesting equilibrium between the free ligand HL form and the complex $[\text{Zn}(\text{L})\text{Cl}_2]^-$ form through a ligand dissociation/recoordination process associated with proton-shuttling in solutions, and more importantly, this dynamic behavior is concentration-

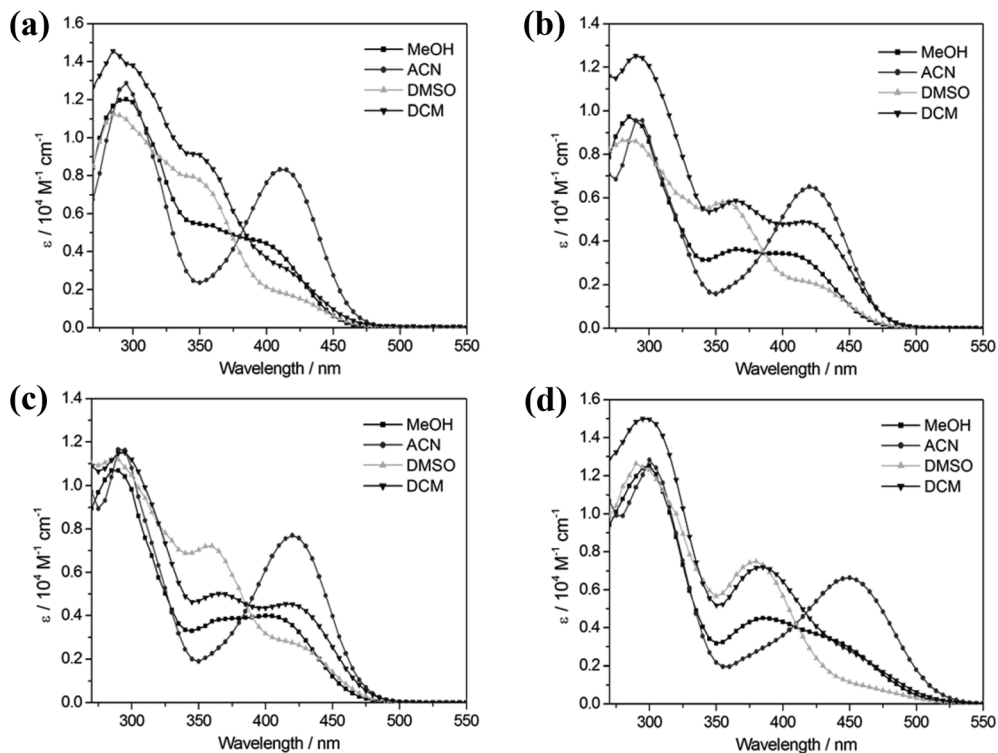


Fig. 7 UV-vis absorption spectra of (a–d) 1–4 in various solvents (100 μM) at room temperature.

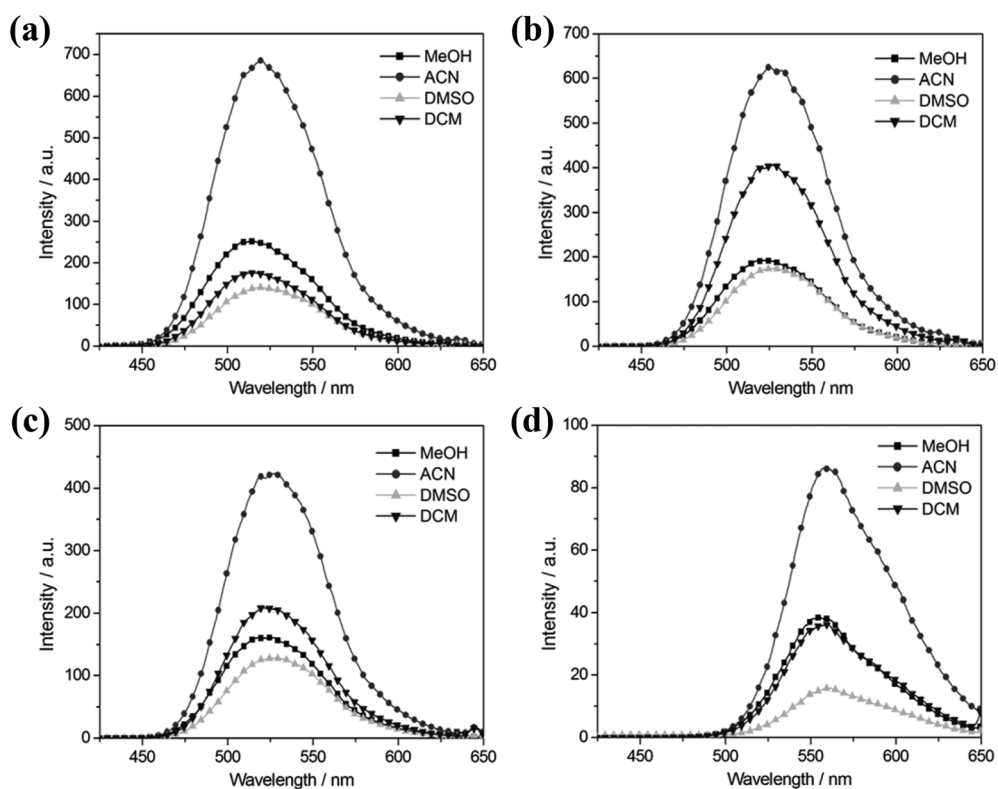


Fig. 8 Fluorescence spectra of (a–d) 1–4 in various solvents (100 μM) at room temperature.

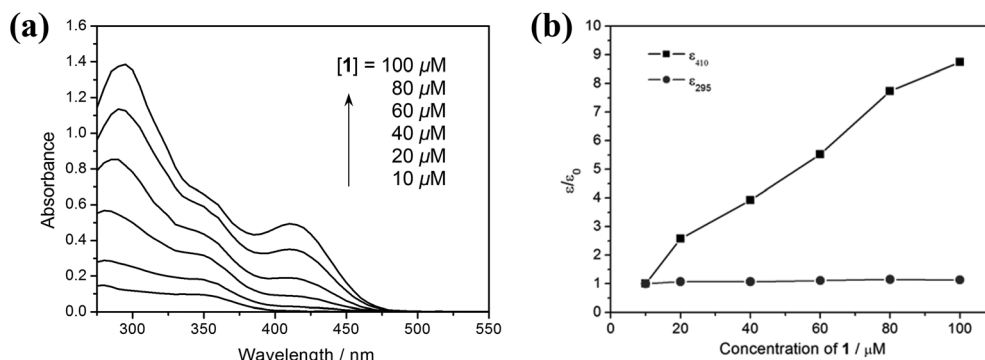


Fig. 9 (a) Concentration dependence (10–100 μM) of UV-vis absorption spectra of **1** in ACN at room temperature. (b) Plots of the ratio of the molar absorption coefficient of the IL (ϵ_{295} , ●) and MLCT (ϵ_{410} , ■) bands against concentration of **1**.

dependent. Thus, further photophysical studies for **1** have been performed in ACN solvent at room temperature to illustrate the influence of concentration on the photophysical properties of ionic zinc–salicylideneimine compounds. Indeed, electronic absorption spectra of **1** in ACN solvent are concentration dependent. A progressive change of spectral features between 390 and 460 nm is observed in the range of concentration between 1.0×10^{-4} and 1.0×10^{-5} M (Fig. 9a). Starting from dilute solutions and proceeding to higher concentrations, a continuous evolution of the defined peak at 410 nm can be observed. Fig. 9b shows plots of the ratio of the molar absorption coefficient (ϵ/ϵ_0) of the IL (ϵ_{295}) and the MLCT (ϵ_{410}) bands against concentration of **1**. The ϵ/ϵ_0 ratio for ϵ_{295} is approximately equal to 1 for compound **1** at different concentrations, while that for ϵ_{410} , in comparison, increases significantly with the increase in concentration of **1**. For example, when the concentration of **1** is increased from 10 μM to 100 μM , *i.e.* a 10-fold increase in concentration, the ϵ_{295} value remains approximately unchanged ($\epsilon/\epsilon_0 \approx 1$), but the ϵ_{410} value becomes ~ 8.7 -fold large in size ($\epsilon/\epsilon_0 \approx 8.7$). In other words, the absorbance of the IL (A_{295}) band obeys Beer's Law, with a linear relationship to the concentration of **1**, while that of the MLCT (A_{410}) band does not. This phenomenon unambiguously indicates that in a more concentrated solution the dynamic equilibrium shifts to the direction favoring the formation of the complex $[\text{Zn}(\text{L})\text{Cl}_2]^-$ form rather than the free ligand HL form, since the ϵ_{410} value of the MLCT band is directly related to the amount of the $[\text{Zn}(\text{L})\text{Cl}_2]^-$ species while the ϵ_{295} value of the IL band is related to the ligand. This consists with the results from the ^1H NMR studies mentioned above.

The fluorescence response upon varying the concentration of **1** in ACN solvent, in the above investigated range of concentrations, is rather variable in terms of related intensities and reflects the changes observed in electronic absorption spectra (Fig. 10). The change in intensity is approximately a linear relationship with the concentration of **1**.

Cation-exchange reaction of **1** with NET_4Cl

As shown in Fig. 2, the solid-state structures of compounds **1–4** indicate that the ammonium proton strongly interacts with the phenolato oxygen through noticeable hydrogen-bonding

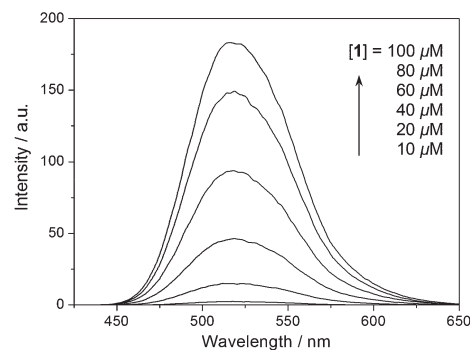
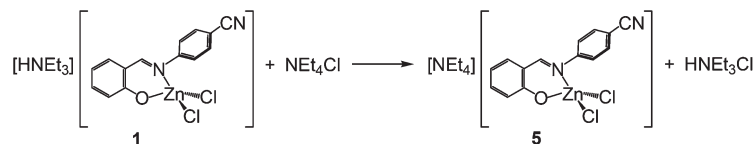


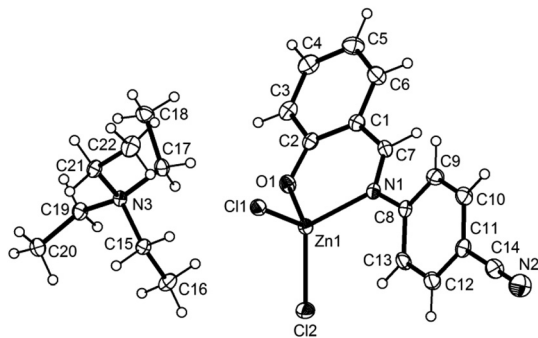
Fig. 10 Fluorescence spectra of **1** in the range of concentration between 1.0×10^{-4} and 1.0×10^{-5} M in ACN solvent at room temperature ($\lambda_{\text{ex}} = 400$ nm).

interactions ($d(\text{N}\cdots\text{O}) = 2.773(7)\text{--}2.8275(16)$ Å, Table 2), offering an opportunity to shift the proton from the triethylammonium group to the phenolate group directly. To understand the importance of the ammonium proton, the tetraethylammonium (NET_4^+) cation is chosen to replace the triethylammonium (HNET_3^+) cation. When treating $[\text{HNET}_3][\text{Zn}(\text{sal}^{\text{H}}\text{-4-CN})\text{Cl}_2]$ (**1**) with NET_4Cl , the ion-exchange product $[\text{NET}_4][\text{Zn}(\text{sal}^{\text{H}}\text{-4-CN})\text{Cl}_2]$ (**5**) is isolated and structurally characterized (Scheme 3). Indeed, the ^1H NMR spectrum of **5** in $\text{DMSO-}d_6$ ($\approx 2.0 \times 10^{-2}$ M) shows the presence of only one set of sharp resonances with the expected multiplicity, according to its molecular structure, in the aromatic region assigning to the anionic Zn–salicylideneimine species; no signals belonging to the free $\text{Hsal}^{\text{H}}\text{-4-CN}$ ligand are observed (Fig. 3). As expected, these ^1H NMR characteristics are independent of the concentration of **5**, as ^1H NMR signals remain roughly unaltered in the explorable range of concentrations (Fig. S9†). This unambiguously indicates that compound **5** does not dissociate in solution and the lack of ammonium proton protects the complex form from ligand dissociation. In other words, the dissociation/recoordination process for **1–4** in solution is mostly driven by the shuttle of proton between the triethylammonium and the phenolate groups.

The solid-state structure of **5** has been determined by single-crystal X-ray diffraction analysis (Fig. 11). The asymmetric unit contains a tetraethylammonium cation, NET_4^+ , and



Scheme 3 Synthesis of 5.

Fig. 11 Molecular structure and atomic numbering scheme of $[\text{NEt}_4][\text{Zn}(\text{sal}^{\text{H}}\text{-4-CN})\text{Cl}_2]$ (**5**).

an anionic Zn–salicylideneimine counterpart, $[\text{Zn}(\text{sal}^{\text{H}}\text{-4-CN})\text{Cl}_2]^-$. Compared with **1**, the NEt_4^+ cationic part attracts the $[\text{Zn}(\text{sal}^{\text{H}}\text{-4-CN})\text{Cl}_2]^-$ anionic part through only electrostatic forces; there is no N–H...O hydrogen-bonding interaction due to the lack of ammonium proton. The molecular structure of **5** shows the zinc atom in a four-coordinate distorted tetrahedral geometry, with one azomethine and one phenolato groups from one $\text{sal}^{\text{H}}\text{-4-CN}$ ligand and two chloro ligands. The bond lengths of Zn–O, Zn–N, and Zn–Cl are 1.9345(16), 2.0360(19), and 2.2418(7)–2.2646(6) Å, respectively, and the bite angle of O–Zn–N is 95.42(7)° while the dihedral angle between the benzonitrile phenyl ring and the salicylideneimine phenyl ring is 22.5° (Table S1†).

The solution-phase optical absorption spectra (>270 nm) of **5** in various solvents (DMSO, ACN, MeOH, DCM, 1.0×10^{-4} M, Fig. 12a and Table 4) all consist of an intense absorption band centered at around 300 nm involving principally intraligand $\pi \rightarrow \pi^*$ transition and a moderately intense structure centered

at 395–415 nm possibly relating to both the ligand and the metal center, *i.e.* $[\text{d}^{10}(\text{Zn}) \rightarrow \pi^*(\text{azoimine})]$ MLCT character.²⁵

Fluorescence studies of **5**, in the same range of solvents, indicate the presence of an unstructured fluorescence band with a maximum at 518 ± 2 nm (Fig. 12b and Table 4), which is similar to that of **1**. Interestingly, the fluorescence band for **5** is stronger in intensity than those shown by **1** in the same kind of solvents with the same concentration. This is mostly attributed to the non-dissociative feature of **5**. Furthermore, like **1–4**, the fluorescent band ($\lambda_{\text{max}} = 531$ nm) of **5** in the solid phase is red-shifted by 13 ± 2 nm, but substantially more intense (*ca.* 2.5–8 fold), compared with that in solution phases.

Conclusions

In summary, we have successfully synthesized a series of ionic zinc–salicylideneimine compounds, $[\text{HNEt}_3][\text{Zn}(\text{L})\text{Cl}_2]$ (L = $\text{sal}^{\text{H}}\text{-4-CN}$, $\text{sal}^{\text{Cl}}\text{-4-CN}$, $\text{sal}^{\text{Br}}\text{-4-CN}$, and $\text{sal}^{\text{OMe}}\text{-4-CN}$). These zinc materials exhibit intense fluorescence properties in both solution and solid phases. However, they are not stable in solution. Detailed ^1H NMR and optical spectroscopic studies indicate the occurrence of ligand dissociation and recoordination in these fluorescent zinc materials in solution, leading to a dynamic equilibrium between the complexed zinc–salicylideneimine species, $[\text{Zn}(\text{L})\text{Cl}_2]^-$, and the free salicylideneimine ligand, HL. The degree of ligand dissociation is found to be related to the solvent, the concentration, and the substitution of the salicylidene ring. However, with only one set of proton resonances observed in the ^1H NMR spectrum for the ion-exchange product $[\text{NEt}_4][\text{Zn}(\text{sal}^{\text{H}}\text{-4-CN})\text{Cl}_2]$, it is clear that

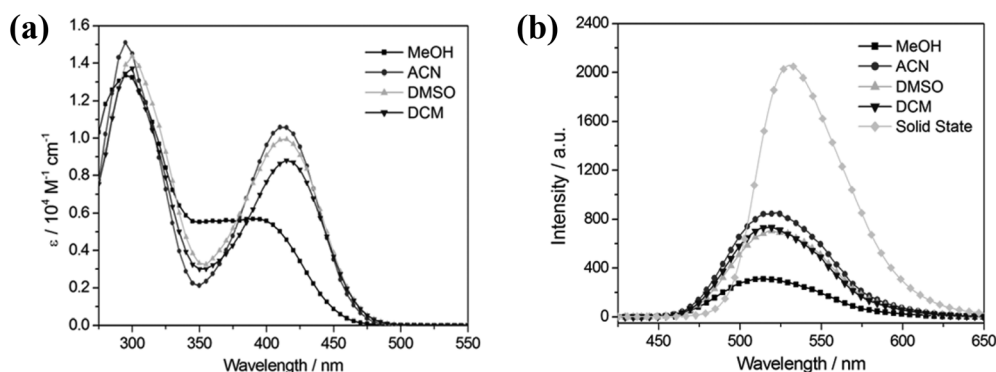


Fig. 12 (a) UV-vis absorption spectra of **5** in various solvents (100 μM) at room temperature. (b) Fluorescence spectra of **5** in various solvents (100 μM) and in solid-state at room temperature.

the lack of ammonium proton would protect the complex $[Zn(L)Cl_2]^-$ form from ligand dissociation.

Acknowledgements

We are grateful to Academia Sinica and the National Science Council of Taiwan for financial support.

References

- 1 K. C. Gupta and A. K. Sutar, *Coord. Chem. Rev.*, 2008, **252**, 1420–1450.
- 2 (a) E. Sinn and C. M. Harris, *Coord. Chem. Rev.*, 1969, **4**, 391–422; (b) D. A. Atwood and M. J. Harvey, *Chem. Rev.*, 2001, **101**, 37–52; (c) H. Houjou, A. Iwasaki, T. Ogihara, M. Kaneshiro, S. Akabori and K. Hiratani, *New J. Chem.*, 2003, **27**, 886–889; (d) N. Yoshida, K. Ichikawa and M. Shiro, *J. Chem. Soc., Perkin Trans. 2*, 2000, 17–26; (e) B. J. McNelis, L. C. Nathan and C. J. Clark, *J. Chem. Soc., Dalton Trans.*, 1999, 1831–1834; (f) N. Yoshida, H. Oshio and T. Ito, *Chem. Commun.*, 1998, 63–64.
- 3 (a) C. J. Whiteoak, G. Salassa and A. W. Kleij, *Chem. Soc. Rev.*, 2012, **41**, 622–631; (b) E. C. Escudero-Adán, J. Benet-Buchholz and A. W. Kleij, *Inorg. Chem.*, 2007, **46**, 7265–7267; (c) M. Oh and C. A. Mirkin, *Angew. Chem., Int. Ed.*, 2006, **45**, 5492–5494; (d) M. Braun, A. Hahn, M. Engelmann, R. Fleischer, W. Frank, C. Krysch, S. Haremza, K. Kürschner and R. Parker, *Chem.-Eur. J.*, 2005, **11**, 3405–3412.
- 4 (a) S. Akine, T. Taniguchi and T. Nabeshima, *J. Am. Chem. Soc.*, 2006, **128**, 15765–15774; (b) H.-J. Kim, W. Kim, A. J. Lough, B. M. Kim and J. Chin, *J. Am. Chem. Soc.*, 2005, **127**, 16776–16777; (c) Z. Lu, M. Yuan, F. Pan, S. Gao, D. Zhang and D. Zhu, *Inorg. Chem.*, 2006, **45**, 3538–3548; (d) X.-X. Zhou, H.-C. Fang, Y.-Y. Ge, Z.-Y. Zhou, Z.-G. Gu, X. Gong, G. Zhao, Q.-G. Zhan, R.-H. Zeng and Y.-P. Cai, *Cryst. Growth Des.*, 2010, **10**, 4014–4022; (e) X.-X. Zhou, Y.-P. Cai, S.-Z. Zhu, Q.-G. Zhan, M.-S. Liu, Z.-Y. Zhou and L. Chen, *Cryst. Growth Des.*, 2008, **8**, 2076–2079.
- 5 (a) N. Madhavan, C. W. Jones and M. Weck, *Acc. Chem. Res.*, 2008, **41**, 1153–1165; (b) E. N. Jacobsen, *Acc. Chem. Res.*, 2000, **33**, 421–431; (c) L. Canali and D. C. Sherrington, *Chem. Soc. Rev.*, 1999, **28**, 85–93; (d) M. D. Jones, M. G. Davidson, C. G. Keir, L. M. Hughes, M. F. Nahon and D. C. Apperley, *Eur. J. Inorg. Chem.*, 2009, 635–642; (e) J. Park, K. Lang, K. A. Abboud and S. Hong, *J. Am. Chem. Soc.*, 2008, **130**, 16484–16485; (f) N. C. Gianneschi, P. A. Bertin, S. T. Nguyen, C. A. Mirkin, L. N. Zakharov and A. L. Rheingold, *J. Am. Chem. Soc.*, 2003, **125**, 10508–10589; (g) P. Sutra and D. Brunel, *Chem. Commun.*, 1996, 2485–2486; (h) P. G. Cozzi, A. Papa and A. Umani-Ronchi, *Tetrahedron Lett.*, 1996, **37**, 4613–4616.
- 6 (a) S. Sreedaran, K. S. Bharathi, A. K. Rahiman, L. Jagadish, V. Kaviyaran and V. Narayanan, *Polyhedron*, 2008, **27**, 2931–2938; (b) D.-H. Shi, Z.-L. You, C. Xu, Q. Zhang and H.-L. Zhu, *Inorg. Chem. Commun.*, 2007, **10**, 404–406.
- 7 (a) H. Görner, S. Khanra, T. Weyhermüller and P. Chaudhuri, *J. Phys. Chem. A*, 2006, **110**, 2587–2594; (b) Q. Peng, M. Xie, Y. Huang, Z. Lu and Y. Cao, *Macromol. Chem. Phys.*, 2005, **206**, 2373–2380; (c) M. Prabhakar, P. S. Zacharias and S. K. Das, *Inorg. Chem.*, 2005, **44**, 2585–2587; (d) C.-M. Che, S.-C. Chan, H.-F. Xiang, M. C. W. Chan, Y. Liu and Y. Wang, *Chem. Commun.*, 2004, 1484–1485; (e) J. T. Mitchell-Koch and A. S. Borovik, *Chem. Mater.*, 2003, **15**, 3490–3495; (f) P. G. Cozzi, L. S. Dolci, A. Garelli, M. Montalti, L. Prodi and N. Zaccheroni, *New J. Chem.*, 2003, **27**, 692–697.
- 8 (a) M. E. Germain and M. J. Knapp, *J. Am. Chem. Soc.*, 2008, **130**, 5422–5423; (b) M. E. Germain and M. J. Knapp, *Inorg. Chem.*, 2008, **47**, 9748–9750; (c) M. E. Germain, T. R. Vargo, P. G. Khalifah and M. J. Knapp, *Inorg. Chem.*, 2007, **46**, 4422–4429.
- 9 (a) K.-L. Kuo, C.-C. Huang and Y.-C. Lin, *Dalton Trans.*, 2008, 3889–3898; (b) H.-C. Lin, C.-C. Huang, C.-H. Shi, Y.-H. Liao, C.-C. Chen, Y.-C. Lin and Y.-H. Liu, *Dalton Trans.*, 2007, 781–791; (c) K.-H. Chang, C.-C. Huang, Y.-H. Liu, Y.-H. Hu, P.-T. Chou and Y.-C. Lin, *Dalton Trans.*, 2004, 1731–1738.
- 10 (a) G. Consiglio, S. Failla, P. Finocchiaro, I. P. Oliveri and S. di Bella, *Dalton Trans.*, 2012, **41**, 387–395; (b) I. P. Oliveri, G. Maccarrone and S. di Bella, *J. Org. Chem.*, 2011, **76**, 8879–8884; (c) G. Consiglio, S. Failla, P. Finocchiaro, I. P. Oliveri, R. Purrello and S. di Bella, *Inorg. Chem.*, 2010, **49**, 5134–5142; (d) G. Consiglio, S. Failla, I. P. Oliveri, R. Purrello and S. di Bella, *Dalton Trans.*, 2009, 10426–10428; (e) S. di Bella, G. Consiglio, S. Sortino, G. Giancane and L. Valli, *Eur. J. Inorg. Chem.*, 2008, 5228–5234; (f) S. di Bella, G. Consiglio, G. La Spina, C. Oliva and A. Cricenti, *J. Chem. Phys.*, 2008, **129**, 114704; (g) S. di Bella, N. Leonardi, G. Consiglio, S. Sortino and I. Fragalà, *Eur. J. Inorg. Chem.*, 2004, 4561–4565.
- 11 (a) F. Song, C. Wang, J. M. Falkowski, L. Ma and W. Lin, *J. Am. Chem. Soc.*, 2010, **132**, 15390–15398; (b) J. Heo, Y.-M. Jeon and C. A. Mirkin, *J. Am. Chem. Soc.*, 2007, **129**, 7712–7713; (c) Y.-M. Jeon, J. Heo and C. A. Mirkin, *J. Am. Chem. Soc.*, 2007, **129**, 7480–7481; (d) R. Kitaura, G. Onoyama, H. Sakamoto, R. Matsuda, S.-i. Noro and S. Kitagawa, *Angew. Chem., Int. Ed.*, 2004, **43**, 2684–2687; (e) A. Lalehzari, J. Desper and C. J. Levy, *Inorg. Chem.*, 2008, **47**, 1120–1126.
- 12 (a) M. Kuil, I. M. Puijk, A. W. Kleij, D. M. Tooke, A. L. Spek and J. N. H. Reek, *Chem.-Asian J.*, 2009, **4**, 50–57; (b) A. W. Kleij, *Chem.-Eur. J.*, 2008, **14**, 10520–10529; (c) S. J. Wezenberg, E. C. Escudero-Adán, J. Benet-Buchholz and A. W. Kleij, *Inorg. Chem.*, 2008, **47**, 2925–2927; (d) A. W. Kleij, M. Kuil, D. M. Tooke, A. L. Spek and J. N. H. Reek, *Inorg. Chem.*, 2007, **46**, 5829–5831; (e) A. W. Kleij, M. Kuil, D. M. Tooke, M. Lutz, A. L. Spek and J. N. H. Reek, *Chem.-Eur. J.*, 2005, **11**, 4743–4750.

- 13 (a) C. Zhu, G. Yuan, X. Chen, Z. Yang and Y. Cui, *J. Am. Chem. Soc.*, 2012, **134**, 5085–8061; (b) C. Zhu, W. Xuan and Y. Cui, *Dalton Trans.*, 2012, **41**, 3928–3932; (c) G. Li, C. Zhu, X. Xi and Y. Cui, *Chem. Commun.*, 2009, 2118–2120; (d) G. Li, W. Yu, J. Ni, T. Liu, Y. Liu, E. Sheng and Y. Cui, *Angew. Chem., Int. Ed.*, 2008, **47**, 1245–1249; (e) G. Li, W. Yu and Y. Cui, *J. Am. Chem. Soc.*, 2008, **130**, 4852–4583.
- 14 (a) S.-H. Cho, B. Ma, S. T. Nguyen, J. T. Hupp and T. E. Albrecht-Schmitt, *Chem. Commun.*, 2006, 2563–2565; (b) S.-S. Sun, C. L. Stern, S. T. Nguyen and J. T. Hupp, *J. Am. Chem. Soc.*, 2004, **126**, 6314–6326.
- 15 (a) P. W. Roesky, A. Bhunia, Y. Lan, A. K. Powell and S. Kureti, *Chem. Commun.*, 2011, **47**, 2035–2037; (b) A. Bhunia, P. W. Roesky, Y. Lan, G. E. Kostakis and A. K. Powell, *Inorg. Chem.*, 2009, **48**, 10483–10485.
- 16 (a) Z. Xu, J. Yoon and D. R. Spring, *Chem. Soc. Rev.*, 2010, **39**, 1996–2006; (b) S. Kim, J. Y. Noh, K. Y. Kim, J. H. Kim, H. K. Kang, S.-W. Nam, S. H. Kim, S. Park, C. Kim and J. Kim, *Inorg. Chem.*, 2012, **51**, 3597–3602; (c) R. Pandey, P. Kumar, A. K. Singh, M. Shahid, P.-z. Li, S. K. Singh, Q. Xu, A. Misra and D. S. Pandey, *Inorg. Chem.*, 2011, **50**, 3189–3197; (d) Y. Dong, J. Li, X. Jiang, F. Song, Y. Cheng and C. Zhu, *Org. Lett.*, 2011, **13**, 2252–2255.
- 17 (a) X. Zhou, B. Yu, Y. Guo, X. Tang, H. Zhang and W. Liu, *Inorg. Chem.*, 2010, **49**, 4002–4007; (b) S. Wang, G. Men, L. Zhao, Q. Hou and S. Jiang, *Sens. Actuators, B*, 2010, **145**, 826–831; (c) N. Li, Y. Xiang, X. Chen and A. Tong, *Talanta*, 2009, **79**, 327–332; (d) L. Gao, Y. Wang, J. Wang, L. Huang, L. Shi, X. Fan, Z. Zou, T. Yu, M. Zhu and Z. Li, *Inorg. Chem.*, 2006, **45**, 6844–6850; (e) J. Dessingou, R. Joseph and C. P. Rao, *Tetrahedron Lett.*, 2005, **46**, 7969–7971.
- 18 (a) V. Liuzzo, W. Oberhauser and A. Pucci, *Inorg. Chem. Commun.*, 2010, **13**, 686–688; (b) C. R. Bhattacharjee, G. Das, P. Mondal and N. V. S. Rao, *Polyhedron*, 2010, **29**, 3089–3096; (c) H.-J. Son, W.-S. Han, J.-Y. Chun, B.-K. Kang, S.-N. Kwon, J. Ko, S. J. Han, C. Lee, S. J. Kim and S. O. Kang, *Inorg. Chem.*, 2008, **47**, 5666–5676; (d) C. Ma, A. Lo, A. Abdolmaleki and M. J. MacLachlan, *Org. Lett.*, 2004, **6**, 3841–3844; (e) M. La Deda, M. Ghedini, I. Aiello and A. Grisolia, *Chem. Lett.*, 2004, 1060–1061; (f) P. Wang, Z. Hong, Z. Xie, S. Tong, O. Wong, C.-C. Lee, N. Wong, L. Hung and S. Lee, *Chem. Commun.*, 2003, 1664–1665.
- 19 (a) M. Cano, L. Rodríguez, J. C. Lima, F. Pina, A. Dalla Cort, C. Pasquini and L. Schiaffino, *Inorg. Chem.*, 2009, **48**, 6229–6235; (b) A. Dalla Cort, L. Mandolini, C. Pasquini, K. Rissanen, L. Russo and L. Schiaffino, *New J. Chem.*, 2007, **31**, 1633–1638; (c) C. T. L. Ma and M. J. MacLachlan, *Angew. Chem., Int. Ed.*, 2005, **44**, 4178–4182.
- 20 A. Altomare, G. Cascarano, C. Giacovazzo and A. Guagliardi, *SIR92: A program for crystal structure solution*, *J. Appl. Crystallogr.*, 1993, **26**, 343–350.
- 21 G. M. Sheldrick, *SHELX-97 (including SHELXS and SHELXL)*, University of Göttingen, Göttingen, Germany, 1997.
- 22 WINGX: L. J. Farrugia, *J. Appl. Crystallogr.*, 1999, **32**, 837–838.
- 23 L. R. Snyder, *J. Chromatogr.*, 1974, **92**, 223–234.
- 24 K. R. Edelman and B. J. Holliday, *Inorg. Chem.*, 2010, **49**, 6787–6789.
- 25 D. Das, B. G. Chand, K. K. Sarker, J. Dinda and C. Sinha, *Polyhedron*, 2006, **25**, 2333–2340.
- 26 S. di Bella, I. Fragalà, I. Ledoux, M. A. Diaz-Garcia and T. J. Marks, *J. Am. Chem. Soc.*, 1997, **119**, 9550–9557.
- 27 S. di Bella, I. Fragalà, I. Ledoux and T. J. Marks, *J. Am. Chem. Soc.*, 1995, **117**, 9481–9485.
- 28 S. Basak, S. Sen, C. Marschner, J. Baumgartner, S. R. Batten, D. R. Turner and S. Mitra, *Polyhedron*, 2008, **27**, 1193–1200.
- 29 T. Yu, W. Su, W. Li, Z. Hong, R. Hua, M. Li, B. Chu, B. Li, Z. Zhang and Z. Z. Hu, *Inorg. Chim. Acta*, 2006, **359**, 2246–2251.
- 30 S. Sreedaran, K. S. Bharathi, A. K. Rahiman, L. Jagadish, V. Kaviyaran and V. Narayanan, *Polyhedron*, 2008, **27**, 2931–2938.
- 31 K. R. Krishnapriya, D. Saravanakumar, P. Arunkumar and M. Kandaswamy, *Spectrochim. Acta, Part A*, 2008, **69**, 1077–1081.
- 32 A. P. de Silva, H. Q. N. Gunaratne, T. Gunnlaugsson, A. J. M. Huxley, C. P. McCoy, J. T. Rademacher and T. E. Rice, *Chem. Rev.*, 1997, **97**, 1515–1566.
- 33 N. J. Williams, W. Gan, J. H. Reibenspies and R. D. Hancock, *Inorg. Chem.*, 2009, **48**, 1407–1415.
- 34 L. Chen, J. Qiao, J. Xie, L. Duan, D. Zhang, L. Wang and Y. Qiu, *Inorg. Chim. Acta*, 2009, **362**, 2327–2333.